Synthesis and evaluation of gold nanoparticle-modified polyelectrolyte capsules under microwave irradiation for remotely controlled release for cargo

Loretta L. del Mercato,[a]† Edgar Gonzalez,[b] Azhar Z. Abbasi,[a] Wolfgang J. Parak,[*a] Victor Puntes[§b]

[a] Fachbereich Physik and Wissenschaftliches Zentrum für Materialwissenschaften, Philipps Universität Marburg, Marburg, Germany
[b] Institut Català de Nanotecnologia, Barcelona, Spain, and Institut Català de Recerca i Estudis Avançats (ICREA), Barcelona, Spain
† Current address: Nanoscience Institute – CNR, National Laboratory of Nanotechnology (NNL), Lecce, Italy

* wolfgang.parak@physik.uni-marburg.de
§ Victor.Puntes.icn@uab.es

Supporting Information

I) Long term motivation

Polyelectrolyte capsules are fabricated by the stepwise layer-by-layer (LbL) deposition of oppositely charged polymers around a charged spherical surface. [1] The multilayer build-up is electrostatically driven via the surface charge reversal which occurs after each adsorption step. [2] Once the desired LbL composition is obtained, the original template can be removed to obtain hollow polymeric capsules. [3, 4] Since the layers of polyelectrolyte microcapsules are held together primarily by electrostatic forces, charged nanoparticles (NPs) can be integrated into the polyelectrolyte network. [5-7] Depending on the type of incorporated NPs, the resulting NP-modified capsules can be responsive to external physical stimuli such as magnetism, ultrasound and microwave irradiation. [8]

For instance, light irradiation has been employed to remotely open the wall of polymer capsules modified with metal NPs. Capsules with silver or gold NPs in their wall could be opened upon laser irradiation as a result of the temperature increase of the metal NPs upon light absorption. The viability of cells after photo-activated release has been investigated to probe for side effects.

[9] The obtained data have demonstrated the possibility to release cargo molecules into the cytosol of living cells without significantly impairing the cell viability on the time scale of hours. [9] Notably, this method allows for the controlled opening of individual capsules in single cells. Due to high absorption of light by tissue this approach is mostly suitable for *in vitro* studies. In particular it has been employed for time-resolved investigation of stimulated reactions inside living cells. [10]

Magnetic force has been used to localize and release encapsulated material from capsules modified with magnetic NPs. [11-13] For example, Fe-based NPs have been embedded within the walls of polyelectrolyte capsules. [11, 13] Upon application of external magnetic field gradients the capsules could be locally enriched at the designated target region. Dependent of the size of the NPs application of an oscillating magnetic field causes heat via the hysteresis cycle of by rotation of the NPs, which has been demonstrated to lead to damaging of the capsule walls. As a result the permeability of the wall was increased and the encapsulated substances were released. [11, 13] Compared to photo-activated release, magnetism has the potential advantage of being applied inside tissues to switch on the unloading of several capsules at the same time.

Ultrasound has been employed to trigger the release of encapsulated material from polyelectrolyte multilayer capsules with both silver and gold NPs in their walls. [14, 15] When the capsules are subjected to ultrasound, cavitation and collapse of microbubbles from dissolved gases occur. The ultrasonic shock waves propagate through the liquid and cause high shear forces between the successive liquid layers. When such shear forces cleave through the membrane of the capsules, the membrane is torn apart and the capsules are destroyed. [14] Notably, sonication was found to destroy both plain and NP-modified capsules. However NP containing capsules responded more sensitive to ultrasound exposure. It was postulated that at low frequency the temperature difference between the NPs and the medium will be in equilibrium, whereas at high frequency only a small portion of the surface will be affected by thermal waves. Similar frequency dependence is applicable to viscous losses, wherein extensive NP motion occurs at low frequency while little movement takes place at high frequencies. Thus, when the capsules were subjected to ultrasound, a morphological change of the capsule wall occurred which resulted in the disruption of the capsule membrane and release of encapsulated species.

In this work we have investigated the behaviour of polyelectrolyte capsules containing Au NPs into their walls under microwave (MW) irradiation in order to establish a method for burst-like release of molecules from numerous capsules. The general concept is depicted in Scheme 1. Capsules containing a fluorescent cargo in their cavities were suspended into a tube and exposed to MW irradiation. After MW treatment, the wall of capsules was expected to undergo rupture, and thus inducing the release of the encapsulated substances.

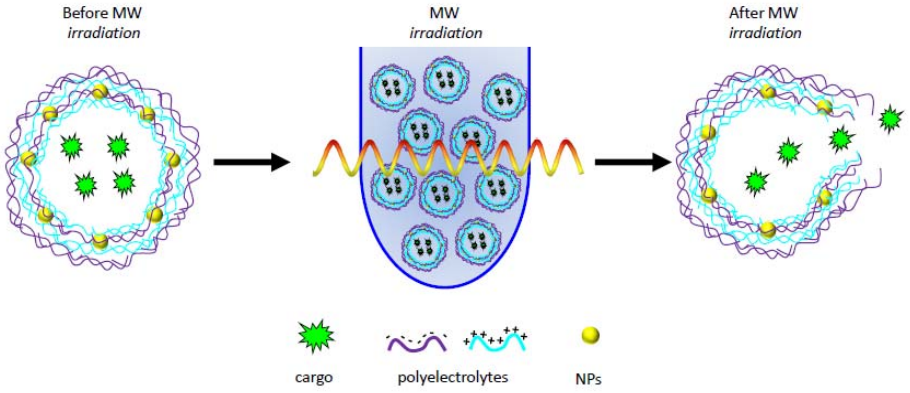

Scheme 1. Schematic representation of the release of substances from Au NP-modified polyelectrolyte capsules. Capsules with Au NPs embedded in their walls were loaded with cargo molecules. After MW treatment, the wall of capsules did undergo rupture and the encapsulated substances were released.

II) Synthesis of microcapsules with and without Au nanoparticles into their wall

II.1) Chemicals
II.2) Synthesis of $CaCO_3$ Particles
II.3) Layer-by-Layer (LbL) assembly of polyelectrolytes on $CaCO_3$ cores and embedding of Au NPs in the wall of capsules

II.1) Chemicals

Poly(sodium 4-styrenesulfonate) (PSS, Mw ~70,000 Da, #243051), poly(allylamine hydrochloride) (PAH, Mw ~56,000 Da, #283223), poly(fluorescein isothiocyanate allylamine hydrochloride) (PAH_{FITC}, Mw ~56,000 Da, #630209), calcium chloride dehydrate ($CaCl_2$, #223506), sodium carbonate (Na_2CO_3, #S7795), ethylenediaminetetraacetic acid (EDTA, #E5134) and dextran (M_w ~2000,000 Da, # 95771) were purchased from Sigma-Aldrich. Citrate-coated gold nanoparticles (NPs) of 20 nm diameter were obtained from BBI/TED Pella (Redding, CA, USA). In order to improve their stability in buffer solution, the adsorbed citrate molecules were replaced by a phosphine (bis(p-sulfonatophenil)phenylphosphine dehydrate, dipotassium salt).[16] The concentration of the Au NPs (20 nm core diameter) was determined by UV/vis spectroscopy by using the molecular extinction coefficient (1.13×10^9 $M^{-1}cm^{-1}$) of their absorption at the plasmon peak.

II.2) Synthesis of $CaCO_3$ Particles

$CaCO_3$ microparticles were precipitated from solutions of calcium chloride ($CaCl_2$) and sodium carbonate (Na_2CO_3) under vigorous stirring. [17] In a typical synthesis, equal volumes (0.615 mL) of aqueous $CaCl_2$ and Na_2CO_3 solutions (0.33 M) were mixed in the presence of 5 mg/mL of

dextran and thoroughly agitated on a magnetic stirrer for 30 s at room temperature. After the agitation, the mixture was left without stirring for 4 min at room temperature. Subsequently, the precipitate was separated from the supernatant by centrifugation (6000 rpm for 5 s) and washed three times with milli-Q water to remove unreacted species. In the last step, the particles were washed with acetone and dried in vacuum. We incorporated dextran in the $CaCO_3$ cores as dissolution of the cores including dextran by addition of EDTA was faster than that of cores without dextran. Naturally, in this way trace of dextran remain in the capsule cavities after core dissolution.

II.3) Layer-by-Layer (LbL) assembly of polyelectrolytes on $CaCO_3$ cores and embedding of Au NPs in the wall of capsules

20 mg of dried $CaCO_3$ particles were weighted and dispersed in a 0.5 M NaCl solution containing the polyanion PSS (2 mg mL^{-1}). The dispersion was continuously shaken for 12 min. The excess polyanion was removed by three centrifugation/washing steps with 1 mL of milli-Q water (6000 rpm for 5 s). Subsequently, 1 mL of a 0.5 M NaCl solution containing the polycation PAH (2 mg mL^{-1}) was added and the dispersion was continuously shaken for 12 min., followed again by three centrifugation/washing steps (6000 rpm for 5 s). This procedure was repeated three times for each polyelectrolyte resulting in the deposition of ten polyelectrolyte layers around the $CaCO_3$ particles.

Two different types of microcapsules were produced: with and without Au NPs in the multilayer wall (Scheme 2). For capsules with Au NPs, the capsules were resuspended in a solution of phosphine-stabilized 20 nm Au NPs (500 µL of 0.045 µM stock) following the deposition of the eighth layer (PAH). The final multilayer composition was $(PSS/PAH)_4AuNP(PSS/PAH)$. For capsules without Au NPs, the final multilayer composition was $(PSS/PAH)_5$.

In a second step, the $CaCO_3$ core was removed by complexation with EDTA buffer. Coated $CaCO_3$ particles were shaken for 2 min. with 1 mL of an EDTA solution (0.2 M, pH 5.0), followed by centrifugation (1200 rpm for 8 min.) and redispersion in 1 mL of a fresh EDTA solution (0.2 M, pH 7.0). We observed that the initial exposure of the microcapsules to a slightly acidic EDTA solution lead to a faster and complete decomposition of the $CaCO_3$ cores compared to their direct exposure to a neutral EDTA solution, as previously reported by others. [13, 14, 18] Then the capsules were washed with 1 mL of neutral EDTA for quickly increasing the pH up to 7.0. To remove the dissolved ions, the thus obtained hollow microcapsules were gently washed five times with 1 mL of fresh milli-Q water (centrifugation at 1200 rpm for 8 min.). The microcapsules were finally stored as suspension in water at 4°C. The microcapsule concentration was estimated in the present case to be $6.70x10^8$ capsules/mL for the capsules with Au NPs in the wall, and $1.12x10^8$ capsules/mL for the control system (capsules without Au NP in the wall). The capsule number per volume was determined by direct counting by a haemocytometer under a microscope. A drop of a diluted solution of capsules was added onto the chamber and the number of capsules in the volume defined by the haemocytometer was counted by using a 20X objective in phase contrast channel.

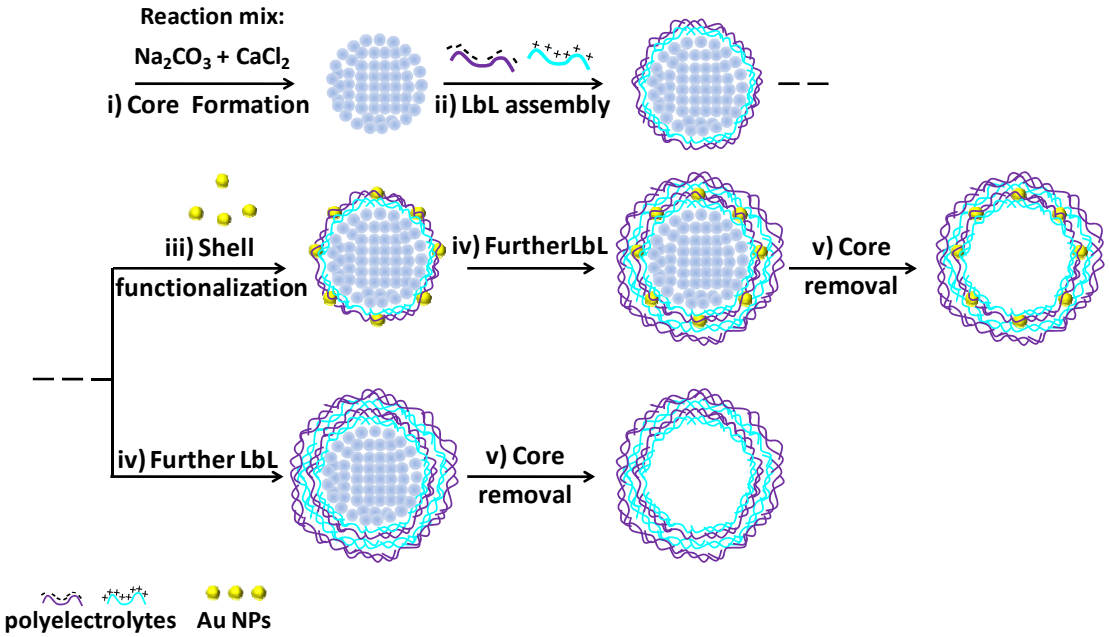

Scheme 2. Schematic illustration of the synthesis of polyelectrolyte capsules with and without Au NPs embedded in the wall. i) A spherical $CaCO_3$ porous template is synthesized by mixing two solutions of Na_2CO_3 and $CaCl_2$. ii) The $CaCO_3$ particle is then coated via consecutive LbL deposition of oppositely charged polyelectrolytes to grow a multilayer polymer wall around the template. iii) The wall is functionalized by loading charged Au NPs onto an oppositely charged layer during the LbL assembly. iv) LbL of polyelectrolytes is repeated to obtain a stable multilayer wall on both capsules with and without Au NPs in the wall. v) The spherical template is removed to obtain a multilayer capsule with and without Au NPs in the walls. Capsules are not drawn to scale. Only few layers of polyelectrolyte and of NPs are shown for sake of clarity.

III) Microwave (MW) irradiation

MW radiation was produced by a house-build customized RF microwave generator at 2.45 GHz. The sample was placed inside the resonating chamber for irradiation. In this condition, and for a sample volume of 1.5 mL, the temperature increases by 1^0C in a radiation time of one minute. The power administrated to the system is 100 mW with a total thermal energy of 6.3 J every minute. In order to irradiate the two capsules systems under the same MW conditions, the stock of capsules with Au NPs (6.70×10^8 capsule/mL) was diluted to 1.12×10^8 capsule/mL, so that both samples had the same capsule concentration. Afterwards an aqueous suspension (1 mL) of capsules with and without NPs containing 1.12×10^8 capsules/mL was placed into the resonating chamber for irradiation. Samples were not shaken to avoid interference with mechanical disruption and an inner temperature probe was used to monitor the temperature variation at the sample position.

IV) Dynamic light scattering (DLS)

Measurements were made with a Malvern ZetaSizer Nano ZS Instrument operating at a light source wavelength of 532 nm and a fixed scattering angle of 173° for detection. Aliquots of 0.8 mL of the colloidal NP solutions were placed into the specific cuvette and the software was arranged with the specific parameters of refractive index and absorption coefficient of the material and solvent viscosity (T = 25 °C; refractive index solvent= 1.33; Au NPs= 0.470; viscosity= 0.8872 cP; absorption = 0.1). DLS allows for determining of the hydrodynamic diameter of colloidal particles. This is the diameter of the equivalent sphere with the same Brownian motion as the analysed sample. The observed differences of the initial diameter between the DLS values of capsules with and without NPs are attributed to the different contrast of the different capsules under the measuring beam but with and without the presence of metallic (plasmonic) NPs.

V) Transmission electron microscopy (TEM)

Polyelectrolyte capsules, with and without Au NPs into the multilayer walls, were analysed by Transmission Electron Microscopy (TEM) after core removal by using a JEOL 3010 TEM operating at an accelerating voltage of 300 kV. A 10 µL drop sample was placed on a Formvar®/carbon coated TEM-grid (300 Mesh 3.05 mm Copper, Plano GmBH) and dried at room temperature before imaging.

VI) Inductive coupled plasma mass spectroscopy (ICP-MS)

The number of Au NPs per capsule has been calculated by measuring the amount of Au ions per capsule as obtained from inductive coupled plasma mass spectroscopy (ICP-MS; Agilent 7500ce). For the ICP-MS measurements 100 µL of capsule sample from the original stock was centrifuge at high speed (14000 rpm) for 10 min. After centrifuge the supernatant was removed and pellet was first digested with 20 µL of 12 M concentrated nitric acid to oxidize the organic coating around the NPs. Then 80 µL of 12 M hydrochloric acid was used to dissolve the Au NPs into Au ions. Concentration of Au determined from ICP-MS measurement was $2x10^{-6}$ mol/mL. We calculated that one Au NP of 20 nm contains $2.4x10^{5}$ atoms of Au. Using this number we calculated the total number of Au NPs in the solution to be $2.4x10^{5}$ times smaller than the total number of Au ions in the solution. The concentration of capsules in stock solution was determined to be $\sim 10^{8}$ capsules per mL, by counting the number of capsules using the microscope in phase contrast mode. At the end the number of Au NPs per capsules was calculated by dividing the concentration of Au NPs by the number capsules in the solution. The obtained value was $7.29x10^{3}$ Au NPs per capsule. The calculation is given in details below.

p refers to nanoparticles
m_{aAu} = mass of 1 Au atom / ion
ρ_{Au} = density of Au
V_{pAu} = Volume of 1 Au NP (diameter 20 nm)
m_{pAu} = mass of 1 Au NP (diameter 20 nm)
N_{aAu} = number of Au atoms in one Au NP
N_{pAu} = refers to the number of Au NPs in the sample solution
N_{Au} = number of detected Au ions within the sample solution

c_{Au} = concentration of Au ions in the sample solution
V = Volume of sample solution
N_{caps} = number of capsules in the sample solution

To calculate the number of Au atoms per 20 nm Au NP firstly we calculated the mass of one Au NP of 20 nm (m_{pAu}) using the following formula: $m_{pAu} = \rho_{Au} \bullet V_{pAu}$. ρ_{Au} is the mass density of Au which is 19.3 g/cm^3. V_{pAu} is the volume of one Au NP calculated using the formula $V_{pAu} = 4/3\ \pi\ r^3$, whereby r = 10 nm is the core radius of one Au NP. The calculated volume V_{pAu} is $4.1x10^{-18}$ cm^3. Using the above given values ρ_{Au} and V_{pAu} , the mass of one Au NP (m_{pAu}) was calculated to be $8.1x10^{-17}$ g. The total mass of one Au atom / ion (m_{aAu}) is $3.2x10^{-22}$ g. The number of Au atoms in one 20 nm Au NP was obtained by dividing the mass of one Au NP (m_{pAu}) by the total atomic mass of Au (m_{aAu}). We found $2.4x10^5$ atoms of Au in one 20 nm Au NP (N_{aAu}).

With ICP-MS measurements we determined the concentration of Au ions in solution after dissolving the Au NPs: $c_{Au.}$ From the Au concentration c_{Au} we got the total number of Au atoms (N_{Au}) within sample by $N_{Au} = c_{Au} \bullet V \bullet N_A$ with the Avogadro number $N_A = 6.02x10^{23}$. The volume of the samples was V = 1 mL. In our experiments we got $c_{Au} = 2x10^{-6}$ mol / 1 mL as result. From this concentration value we got the total number of Au atoms (N_{Au}) in this sample, which was $N_{Au} = 1.21x10^{18}$. Each Au NP contains $2.4x10^5$ (N_{aAu}) Au atoms. Thus the number of Au NPs in the sample solution (N_{pAu}) was calculated by dividing N_{Au} with $2.47x10^5$. This resulted in the value $N_{pAu} = 4.88x10^{12}$.

The number of capsules N_{caps} in the samples was counted to be $N_{caps} = 6.70x10^8$ (this was the original number of capsules/mL in the stock solution). Finally, the number of Au NPs per capsule was obtained by dividing the number of Au NPs (N_{pAu}) by the number of capsules (N_{caps}) in the sample. $N_{pAu}/N_{caps} = 4.88x10^{12} / 6.70x10^8 = 7.29x10^3$.

Two independent ICP-MS measurements were performed onto two samples of capsules containing Au NPs into their walls. The number of nanoparticle/capsule was found to be in the 10^3-10^4 range[1].

References

1. G. Decher, *Science*, 1997, **277**, 1232-1237.
2. G. Decher and J. Schlenoff, *Multilayer Thin Films: Sequential Assembly of Nanocomposite Materials*, Wiley VCH, 2002.
3. E. Donath, G. B. Sukhorukov, F. Caruso, S. A. Davis and H. Möhwald, *Angewandte Chemie International Edition*, 1998, **37**, 2202-2205.

[1] These data are in contrast with previous results reported in a previous work in which FePt NPs were embedded into the walls of polymer capsules (J. Mater. Chem., 2009, 19, 6381–6386). In this previous work we calculated the number of NPs / capsule wrongly.

4. G. B. Sukhorukov, E. Donath, S. Davis, H. Lichtenfeld, F. Caruso, V. I. Popov and H. Möhwald, *Polymers for Advanced Technologies*, 1998, **9**, 759-767.
5. B. Radt, T. A. Smith and F. Caruso, *Advanced Materials*, 2004, **16**, 2184-2189.
6. A. G. Skirtach, A. A. Antipov, D. G. Shchukin and G. B. Sukhorukov, *Langmuir*, 2004, **20**, 6988-6992.
7. M. F. Bedard, D. Braun, G. B. Sukhorukov and A. G. Skirtach, *Acs Nano*, 2008, **2**, 1807-1816.
8. M. F. Bedard, B. G. De Geest, A. G. Skirtach, H. Mohwald and G. B. Sukhorukov, *Adv Colloid Interface Sci*, 2010, **158**, 2-14.
9. A. Muñoz_Javier, P. d. Pino, M. Bedard, A. G. Skirtach, D. Ho, G. Sukhorukov, C. Plank and W. J. Parak, *Langmuir*, 2009, **24**, 12517-12520.
10. R. Palankar, A. Skirtach, O. Kreft, M. Bedard, M. Garstka, K. Gould, H. Mohwald, G. Sukhorukov, M. Winterhalter and S. Springer, *SMALL*, 2009, **5**, 2168-2176.
11. Z. Lu, M. D. Prouty, Z. Guo, V. O. Golub, C. S. Kumar and Y. M. Lvov, *Langmuir*, 2005, **21**, 2042-2050.
12. B. Zebli, A. S. Susha, G. B. Sukhorukov, A. L. Rogach and W. J. Parak, *Langmuir*, 2005, **21**, 4262-4265.
13. S. H. Hu, C. H. Tsai, C. F. Liao, D. M. Liu and S. Y. Chen, *Langmuir*, 2008, **24**, 11811-11818.
14. B. G. De_Geest, A. G. Skirtach, A. A. Mamedov, A. A. Antipov, N. A. Kotov, S. C. De Smedt and G. B. Sukhorukov, *SMALL*, 2007, **3**, 804-808.
15. A. G. Skirtach, B. G. De_Geest, A. Mamedov, A. A. Antipov, N. A. Kotov and G. B. Sukhorukov, *Journal Of Materials Chemistry*, 2007, **17**, 1050-1054.
16. D. Zanchet, C. M. Micheel, W. J. Parak, D. Gerion and A. P. Alivisatos, *Nanoletters*, 2001, **1**, 32-35.
17. D. V. Volodkin, N. I. Larionova and G. B. Sukhorukov, *Biomacromolecules*, 2004, **5**, 1962-1972.
18. S. De Koker, T. Naessens, B. G. De Geest, P. Bogaert, J. Demeester, S. De Smedt and J. Grooten, *Journal of Immunology*, 2010, **184**, 203-211.